Inelastic Electron Tunneling Spectroscopy of a Single Nuclear Spin

F. Delgado[1] and J. Fernández-Rossier[1,2]

[1]*Departamento de Física Aplicada, Universidad de Alicante, San Vicente del Raspeig, 03690 Spain*
[2]*International Iberian Nanotechnology Laboratory, Av. Mestre José Veiga, 4715-310 Braga, Portugal*

(Received 21 December 2010; published 9 August 2011)

Detection of a single nuclear spin constitutes an outstanding problem in different fields of physics such as quantum computing or magnetic imaging. Here we show that the energy levels of a single nuclear spin can be measured by means of inelastic electron tunneling spectroscopy (IETS). We consider two different systems, a magnetic adatom probed with scanning tunneling microscopy and a single Bi dopant in a silicon nanotransistor. We find that the hyperfine coupling opens new transport channels which can be resolved at experimentally accessible temperatures. Our simulations evince that IETS yields information about the occupations of the nuclear spin states, paving the way towards transport-detected single nuclear spin resonance.

DOI: 10.1103/PhysRevLett.107.076804 PACS numbers: 73.23.Hk, 31.30.Gs, 74.55.+v, 75.75.−c

Probing a single nuclear spin represents both the ultimate resolution limit of magnetic resonance imaging and a requirement in quantum computing proposals where the nuclear spin is used as a qubit. The idea of storing and manipulating information in nuclear spins goes back to quantum computing proposals based on P donors in Si [1] and NMR quantum computing [2]. Because of their very small coupling to their environment, the nuclear spin coherence time is expected to be very long but, for the same reason, quantum measurement of a single nuclear spin remains a formidable task. Recent experimental breakthroughs have permitted performing single shot nondestructive measurement of a single nuclear spin by means of optically detected single spin magnetic resonance in NV centers in diamond [3].

In this Letter we propose a setup based on IETS that can probe the spin transitions of a single nuclear spin with a space resolution down to 1 Å, outperforming in this particular regard the optical detection. We exploit the relation between the nuclear spins and the transport properties as proposed in Ref. [4], but without the need of an external microwave field. Our proposal builds on recent progress to probe the spin of a single atom using two different strategies. On one side, STM-IETS [5–11] which allows one to measure the electron spin spectral function of a single magnetic atom [12] weakly coupled to a conducting substrate. On the other side, the fabrication of a silicon nanotransitor where transport occurs through the electronic states of a single dopant [13,14].

In STM-IETS experiments, electrons tunnel between the tip and the conducting substrate going through the magnetic atom. As the bias voltage V is increased, a new conduction channel opens whenever eV is larger than the energy of some internal excitation of the atom. In the case of isolated transition metal atoms with partially full d shell, like Mn, Fe or Co, the only internal excitations available in the range of a few meV are spin excitations associated to the magnetocrystalline anisotropy [7,12]. In the case of the single dopant nanotransistor, the IETS of the electron spin in the donor level could be performed in the cotunneling regime [15].

Exchange coupling to nearby magnetic atoms affects significantly the spin excitation spectrum of the atom under the tip [6,9,10,12]. Hyperfine coupling to the nuclear spin should also result in a modification of the electronic spin spectral function which, in turn, could be probed in IETS provided that the spectral resolution is high enough. Our proposal differs from earlier theoretical works [16,17] which suggest detecting the nuclear spin looking at its influence on the STM current noise spectrum. Their approach is based on previous experiments where electronic spin fluctuations are detected in the current noise spectra [18], not in the conductivity spectra. Probing the spin transitions of a single nuclear spin would yield a completely unambiguous chemical identification of the atom and would be a first step towards transport-based quantum measurement of a single nuclear spin.

The rest of this Letter is organized as follows. We first describe the general theory that relates nuclear spin flips to IETS transport features. Then we consider the archetypical case of a single Mn atom in a Cu_2N surface [5–7,10]. We find that the visibility of the nuclear spin excitations can be enhanced driving the nuclear spin out of equilibrium, but still its detection could not be done above 4 mK, below the recently demonstrated 10 mK experimental limit [19]. We then analyze the case of ^{209}Bi in silicon and we find it is an optimal system to observe single nuclear spin flips at temperatures up to 60 mK.

The electronic spin S and nuclear total angular momentum I are described by a Hamiltonian $\mathcal{H}_0(S, I)$ whose eigenvalues and eigenvectors are denoted by ϵ_M and $|M\rangle = \sum_{I_z,S_z} \Psi_M(I_z, S_z)|I_z\rangle|S_z\rangle$, where $|I_z\rangle|S_z\rangle$ is the basis in which both electronic and nuclear spin have well defined projection along the z axis. The spin mixing coefficients

$\Psi_M(I_z, S_z)$ depend on the specifics of the Hamiltonian, described below, which includes hyperfine coupling, Zeeman splitting and magnetic anisotropy terms. The IETS is sensitive to transitions between states M and M' with excitation energy $\Delta_{M',M} = \epsilon_{M'} - \epsilon_M$. The electronic spin is coupled to electrons in the electrodes, denoted as tip (source) and surface (drain) in the STM (nanotransistor) geometry, through a Kondo-like Hamiltonian [12,20–22]:

$$\mathcal{V} = \sum_{\alpha,\lambda,\lambda',\sigma,\sigma'} T_{\lambda,\lambda',\alpha} \frac{\tau^{(\alpha)}_{\sigma\sigma'}}{2} \hat{S}_\alpha c^\dagger_{\lambda,\sigma} c_{\lambda'\sigma'}, \quad (1)$$

where both electrode conserving and electrode nonconserving exchange couplings are included. The operator $c^\dagger_{\lambda,\sigma}$ creates an electron with spin σ and orbital quantum number $\lambda = \eta, \vec{k}$, where $\eta = T, S$ labels the electrode and $\vec{k}$ the wave vector. The index α runs over $a = x, y, z$, with $\tau^{(a)}$ and $\hat{S}_a$ the Pauli matrices and the atom electronic spin operators, respectively. The $\alpha = 0$ term (with $\tau^{(0)}$ and $\hat{S}_0$ the identity matrix) corresponds to potential scattering. We assume that exchange is momentum independent, spin isotropic and electrode dependent: $T_{\lambda,\lambda',a} \equiv \upsilon_\eta \upsilon_{\eta'} \mathcal{T}$. Here υ_η are dimensionless parameters that account for the different coupling between the magnetic adatom and either the tip or the surface [22,23].

The inelastic current due to electronic-spin assisted tunneling $I_{\rm in}$ can be expressed [12] as a convolution of the electronic spin spectral function:

$$\mathcal{S}(\omega) \equiv \sum_{M,M',a} P_M |\hat{S}^{M,M'}_a|^2 \delta(\hbar\omega - \Delta_{M',M}), \quad (2)$$

where $P_M \equiv P_M(V)$ denotes the average occupation of the state M and $\hat{S}^{M,M'}_a = \langle M|\hat{S}_a|M'\rangle$. The inelastic current can be written as [12,23]:

$$I_{\rm in}(V) = \frac{g_0}{G_0} \sum_{M,M',a} P_M(V) |\hat{S}^{M,M'}_a|^2 i(\Delta_{M,M'} + eV). \quad (3)$$

Here $g_0 \equiv \frac{\pi^2}{4} G_0 \rho_T \rho_S |\mathcal{T} \upsilon_T \upsilon_S|^2$ is the elastic tunneling conductance, $G_0 = 2e^2/h$ is the quantum of conductance and ρ_η the density of states of the η electrode at the Fermi level. The inelastic current associated to a single channel is given by $i(\Delta + eV) = (\mathcal{G}(\Delta + eV) - \mathcal{G}(\Delta - eV))G_0/e$, with $\mathcal{G}(\omega) \equiv \omega(1 - e^{-\beta\omega})^{-1}$ and $\beta = 1/k_B T$. Importantly, $di(\Delta + eV)/dV$ has a step at $eV = \Delta$ that accounts for the characteristic dI/dV line shape. Thus, whenever the bias energy eV exceeds a transition energy between spin states M, M' such that the initial state is occupied, $P_M > 0$, and the electronic spin flip transition is permitted, $\hat{S}^{M,M'}_a \neq 0$, the differential conductance dI/dV has a step and d^2I/dV^2 has a peak (or a valley at negative bias) with a thermal broadening [24] of $\Gamma_{k_B T} \equiv 5.4 k_B T$. Thus, the d^2I/V^2 lineshape should be quite similar to the electronic spin spectral function $\mathcal{S}(eV)$. In the following we assume that the intrinsic broadening of the spin excitations, due for instance to their coupling to the conducting substrate [22,23,25], is negligible compared to $\Gamma_{k_B T}$, as it happens in the case of Mn adatoms in Cu_2N [10,23,25].

The occupation functions $P_M(V)$ can differ substantially from those of equilibrium when the typical time elapsed between inelastic current events is shorter than the spin relaxation time [22,23], as recently observed [10]. We determine the occupation functions P_M by solving a master equation [22,23] that accounts for the dissipative dynamics of the current driven electronic spin interacting with the nuclear spin. Both energy and spin are exchanged between the electrons in the electrodes on one side, and the nuclear and electronic spin of the single atom on the other. The scattering events involve the creation or annihilation of an electron-hole pair either in the same electrode, in which case current is not involved, or in different electrodes. Thus, P_M depends in general on the voltage, the conductance and the temperature [23].

We now address the main question of this Letter: under which conditions would IETS reveal transitions that provide information about the nuclear spin state? We first consider the case of a single Mn adatom in a Cu_2N surface. This system has been widely studied experimentally and theoretically [6,7,10,12,21–23,25,26], but the role of the nuclear spin has been overlooked so far. The single atom electronic spin can be described by means of a spin $S = 5/2$ Hamiltonian,

$$\mathcal{H}_S = DS_z^2 + E(S_x^2 - S_y^2) + g_e \mu_B \vec{B} \cdot \vec{S} \quad (4)$$

where $D = -39$ μeV and $E = 7$ μeV account for the uniaxial and in-plane anisotropy,, respectively, whereas the third term describes the electronic Zeeman coupling. At zero magnetic field, the experimental dI/dV [7] features a step at an energy of $\Delta \simeq 4|D|$ associated to the electronic spin flip between the two ground states which, neglecting E, have $S_z = \pm 5/2$, and the first excited states, with $S_z = \pm 3/2$; see Fig. 1(a). The only stable nuclear isotope of Mn is ^{55}Mn and has a nuclear spin of $I = 5/2$. Then, the electronic-nuclear system has 36 states in total. The hyperfine structure associated to the coupling between I and S has been resolved with EPR and NMR experiments that address ensembles of more than 10^{12} atoms, and can be described by a Heisenberg-type coupling. So, the spin Hamiltonian reads as

$$\mathcal{H}_0(S, I) = \mathcal{H}_S + A\vec{S} \cdot \vec{I}. \quad (5)$$

The strength of the hyperfine coupling A depends both on the nuclear magnetic moment and on the shape of the electronic cloud, which is environment dependent. In the case of Mn, A varies between 0.3 and 1 μeV [27]. Here we take the most favorable case with $A = 1$ μeV. The effect of the hyperfine coupling is to split each of the 6 electronic levels into 6 nuclear branches, as observed in Figs. 1(a) and 1(b). The lowest electronic multiplet corresponds to the $S_z = \pm 5/2$, while the $S_z = \pm 3/2$ and $S_z = \pm 1/2$ branches are found approximately at $4|D|$ and $6|D|$ above.

The discussion can be simplified if we take advantage of the fact that $|D| \gg E, A$ so that the eigenstates of $\mathcal{H}_0(S, I)$ have, to zeroth order in E and A, well defined projection of the electronic (S_z) and nuclear (I_z) spin, although the numerical calculations are done with the exact states. The energies are approximately given by $E_0(S_z, I_z) = DS_z^2 + AS_zI_z + g\mu_B S_z$. We find two kind of transitions: low energy excitations with $\Delta S_z \simeq 0$ and higher energy excitations with $\Delta I_z \simeq 0$, $\Delta S_z = \pm 1$. The weak structure [inset of Fig. 1(c)] seen in the d^2I/dV^2 at small bias $|eV| \simeq |S_zA|$ is related to bias induced changes in the occupation of the different nuclear levels [Fig. 1(d)] rather than to steps in the dI/dV, which are thermally blurred.

In contrast, the electronic spin transitions between the electronic ground states $\pm 5/2$ and the first excited states $\pm 3/2$ that, to zeroth order, conserve the nuclear spin, occur at higher $|eV| \simeq 4|D|$ and have a much stronger signal [Figs. 1(c), 1(d), and 2]. At $B = 0$ their energies are given by $\Delta_\pm(I_z) = 4|D| \mp AI_z$, so the hyperfine coupling splits the electronic spin spectral function into 6 lines separated by $A = \Delta_\pm(I_z) - \Delta_\pm(I_z \pm 1)$. In order to have a thermal broadening smaller than A, k_BT must be reduced down to $\simeq 0.2$ μeV ($T \simeq 2$ mK), which depletes the occupation of the higher energy nuclear states within the electronic ground state and therefore, the visibility of the corresponding spin excitations when the system is in thermal equilibrium. Importantly, the transport electrons drive the system out of equilibrium [10] populating higher energy nuclear spin states, as shown in Fig. 1(d), which makes it possible to resolve the hyperfine structure of the $S_z = \pm 5/2 \rightarrow \pm 3/2$ transition even at $T = 4$ mK, as seen in Fig. 2(a).

In Fig. 2(b) we plot d^2I/dV^2 together with the electronic spin spectral function $\mathcal{S}(eV)$, where the occupations P_M were evaluated at $eV = \Delta_+$ and the delta function replaced by d^2i/dV^2. It is apparent that d^2I/dV^2 and $\mathcal{S}(eV)$ are related. Importantly, the spin spectral function contains information not only about the energy levels of the joint nuclear-electronic spin, but also about the *nonequilibrium* occupations of the states. Thus, the height of the d^2I/dV^2 can be correlated with the occupations of the nuclear spin states. This suggest that IETS-STM might be used as a detector of the strong changes of the occupation of the nuclear spin states in a magnetic resonance experiment, but this issue deserves additional work out of the scope of this Letter.

Nuclear spins with larger hyperfine coupling, like Yb, Er, or Pr [28,29], could be probed with IETS at higher temperatures than Mn. For instance $^{167}Er^{3+}$ in Y_2SiO_5 [28] can have A up to 6 μeV while $^{171}Yb^{3+}$ centers in $KTaO_3$ can present $A \sim 15$ μeV [30]. The case of ^{209}Bi in Si is particularly interesting. This system attracts a lot of interest [31,32] in the context of quantum computing based on the nuclear spin of donors [1] thanks to its extremely large coherence time and larger binding energy, which translates into higher operation temperature [31,32]. Two challenges in building the Kane quantum computer are placing the dopants with atomic precision below the surface, and depositing metallic contacts between them, creating gated nanostructures where the energy spectrum of individual donors can be observed and manipulated by changing the local environment or the position of the donors [13,14].

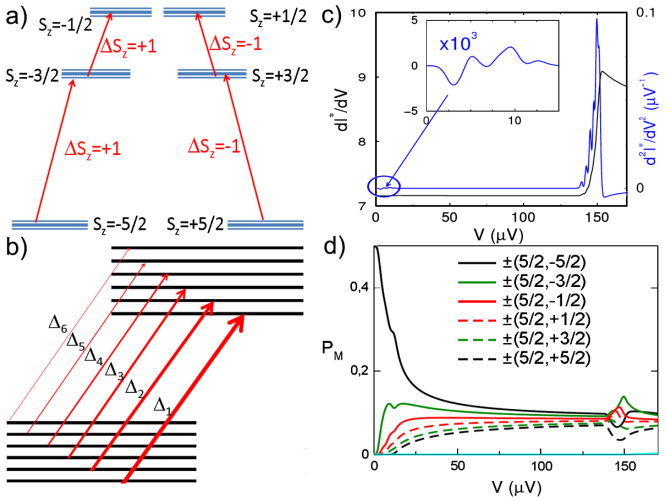

FIG. 1 (color online). (a) Energy level scheme of the $^{55}Mn^{2+}$ adatom on the Cu_2N surface. (b) Detail of the $S_z = 5/2 \rightarrow 3/2$ transition with resolved hyperfine structure. (c) dI^*/dV (black lines) and d^2I^*/dV^2 (blue lines) in the high current regime ($v_T = v_S = 1$) at $T = 4$ mK ($I^* = I/g_0$). Inset: magnified low bias d^2I^*/dV^2. (d) Corresponding occupations of each of the 6 pairs of doubly degenerate electronuclear eigenstates of $\mathcal{H}_0(S, I)$ labeled as S_z, I_z) versus applied bias.

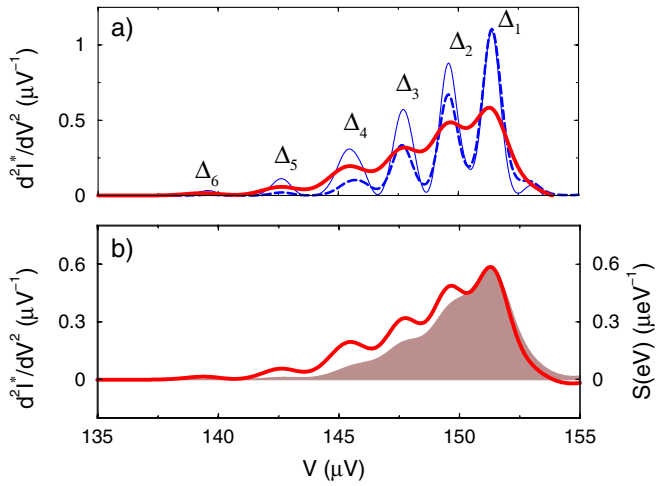

FIG. 2 (color online). Conduction spectrum d^2I^*/dV^2 as a function of applied bias ($I^* = I/g_0$). (a) Spectra for $T = 4$ mK (thick solid line) and $T = 2$ mK (thin solid line) with $v_T = v_S = 1$ (far from thermal equilibrium) and $T = 2$ mK (thick-dashed line) with $10v_T = v_S = 1$ (close to thermal equilibrium). (b) d^2I/dV^2 for $T = 4$ mK and $v_T = v_S = 1$ (solid line) and spin spectral function $S(eV)$ as a function of applied bias (shadow).

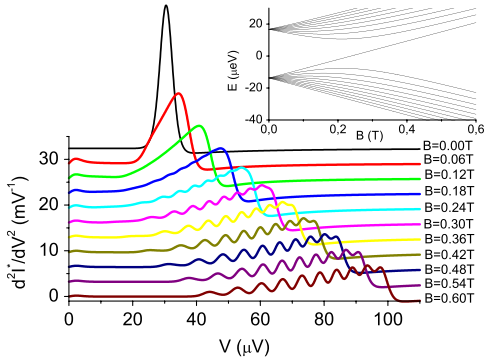

FIG. 3 (color online). Energy spectrum of ^{209}Bi in silicon as a function of applied field and the corresponding $\frac{d^2I^*}{dV^2}$ spectra at $k_BT = 10$ mK.

A single Bi dopant in Si could be probed by single spin IETS-STM, recently demonstrated in semiconductor substrates [11] or in a single dopant Si nanotransistor [13,14], both in the sequential regime, where the dI/dV curve yields the single electron spectral function [33], or in the cotunneling regime, where it provides information about the electronic spin spectral function. The hyperfine coupling between the $I = 9/2$ nuclear spin and the electronic spin of the donor state is quite large, $A = 6.1$ μeV (1.48 GHz) [31,32]. The zero field Hamiltonian $A\vec{I}\cdot\vec{S}$ [31,32] can be diagonalized in terms of the total angular operator F, resulting in two multiplets ($F = 4$, $F = 5$) with energy $E(F) = \frac{A}{2}(F(F+1) - S(S+1) - I(I+1))$. The zero field splitting is as large as $5A \simeq 30$ μeV, which could be resolved in IETS at $k_BT \simeq 60$ mK. The evolution of the spectrum as a function of B is shown in Fig. 3, together with the evolution of the d^2I/dV^2 curves for different values of B at $k_BT = 10$ mK, as measured either with STM or in a nanotransistor in the cotunneling regime. We have assumed that the Anderson model describes the single dopant coupled to the electrodes and, in the Coulomb Blockade regime, a Schrieffer-Wolf transformation maps it to the Kondo coupling [Eq. (1)] used in our calculation [34]. It is apparent that transport permits probing the spin-flip transitions between the Zeeman-split states of the joint electronic-nuclear spin system.

In summary, we propose an experimental approach to probe a single nuclear spin using IETS of the hyperfine structure of the electronic spin excitations, extending thereby the range of applicability of IETS. Our simulations show that this technique yields information about both, energy levels and occupations of the nuclear spin states. We found that driving the occupations of the electronuclear states far from equilibrium improves the visibility of the hyperfine structure of energy levels. Our predictions are based on phenomenological Hamiltonians for the adatom, with parameters extracted for the optimal (stable) isotopes an available experimental data. In the case of a ^{55}Mn adatom probed with a STM, the electronuclear excitations cannot be resolved above 4 mK, bellow the 10 mK state of the art limit. The situation can change by using rare earth atoms with higher hyperfine couplings, where combination of high electronic inelastic signal, associated to its cotunneling nature close to the electron-hole symmetry [23], and high hyperfine coupling will favor its spectral resolution. In the case of a single ^{209}Bi dopant in a Si nanotransistor, the hyperfine structure could be detected at 60 mK, well within the range of current technology.

We acknowledge fruitful discussions with C. Untiedt, C. F. Hirjibehedin and A. F. Otte. This work was supported by MEC-Spain (MAT07-67845, FIS2010-21883-C02-01, Grants JCI-2008-01885 and CONSOLIDER CSD2007-00010) and Generalitat Valenciana (ACOMP/2010/070).

[1] B. Kane, Nature (London) **393**, 133 (1998).
[2] N. A. Gershenfeld *et al.*, Science **275**, 350 (1997).
[3] P. Neumann *et al.*, Science **329**, 542 (2010).
[4] M. Sarovar *et al.*, Phys. Rev. B **78**, 245302 (2008).
[5] A. J. Heinrich *et al.*, Science **306**, 466 (2004).
[6] C. F. Hirjibehedin *et al.*, Science **312**, 1021 (2006).
[7] C. Hirjibehedin *et al.*, Science **317**, 1199 (2007).
[8] A. F. Otte *et al.*, Nature Phys. **4**, 847 (2008).
[9] A. F. Otte *et al.*, Phys. Rev. Lett. **103**, 107203 (2009).
[10] S. Loth *et al.*, Nature Phys. **6**, 340 (2010).
[11] A. A. Khajetoorians *et al.*, Nature (London) **467**, 1084 (2010).
[12] J. Fernández-Rossier, Phys. Rev. Lett. **102**, 256802 (2009).
[13] G. P. Lansbergen *et al.*, Nano Lett. **10**, 455 (2010).
[14] K. Y. Tan *et al.*, Nano Lett. **10**, 11 (2010).
[15] S. De Franceschi *et al.*, Phys. Rev. Lett. **86**, 878 (2001).
[16] G. P. Berman *et al.*, Phys. Rev. Lett. **87**, 097902 (2001).
[17] A. V. Balatsky *et al.*, Phys. Rev. B **73**, 184429 (2006).
[18] Y. Manassen *et al.*, Phys. Rev. Lett. **62**, 2531 (1989).
[19] Y. J. Song *et al.*, Nature (London) **467**, 185 (2010).
[20] J. A. Appelbaum, Phys. Rev. **154**, 633 (1967).
[21] J. Fransson, Nano Lett. **9**, 2414 (2009).
[22] F. Delgado, J. J. Palacios, and J. Fernández-Rossier, Phys. Rev. Lett. **104**, 026601 (2010).
[23] F. Delgado and J. Fernández-Rossier, Phys. Rev. B **82**, 134414 (2010).
[24] J. Lambe and R. C. Jaklevic, Phys. Rev. **165**, 821 (1968).
[25] J.-P. Gauyacq, F. D. Novaes, and N. Lorente, Phys. Rev. B **81**, 165423 (2010).
[26] M. Persson, Phys. Rev. Lett. **103**, 050801 (2009).
[27] W. M. Walsh, J. Jeener, and N. Bloembergen, Phys. Rev. **139**, A1338 (1965).
[28] O. Guillot-Noël *et al.*, Phys. Rev. B **74**, 214409 (2006).
[29] H. Ma and F. Yang, At. Data Nucl. Data Tables **86**, 3 (2004).
[30] W.-L. Feng, H.-G. Liu, and W.-C. Zheng, Spect. Acta Part A: Molec. and Biomol. Spectr. **71**, 559 (2008).
[31] G. W. Morley *et al.*, Nature Mater. **9**, 725 (2010).
[32] R. E. George *et al.*, Phys. Rev. Lett. **105**, 067601 (2010).
[33] J. Fernández-Rossier and R. Aguado, Phys. Rev. Lett. **98**, 106805 (2007).
[34] P. W. Anderson, Phys. Rev. Lett. **17**, 95 (1966).